

AD-A077 364

NAVAL RESEARCH LAB WASHINGTON DC  
A UNIQUE RADIO OCEANOGRAPHIC RADAR. (U)  
NOV 79 J E KENNEY , E J WALSH

F/6 17/9

UNCLASSIFIED

NRL-MR-4086

NASA-L-17098A

NL

| OF |  
ADA  
077364



END  
DATE  
FILMED  
1-80  
DDC





NRL Memorandum Report 4086

AD A 077364

## A Unique Radio Oceanographic Radar

JAMES E. KENNEY

*Advanced Projects Office*

AND

EDWARD J. WALSH

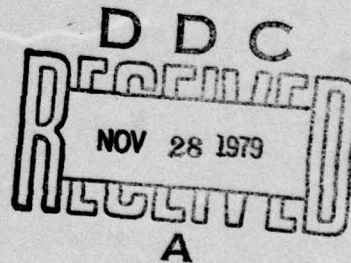
*NASA Wallops Flight Center  
Wallops Island, Virginia 23337*

LEVEL II

November 19, 1979

DDC FILE COPY.

ORIGINAL CONTAINS COLOR PLATES: ALL DDC  
REPRODUCTIONS WILL BE IN BLACK AND WHITE



79 11 28 043

NAVAL RESEARCH LABORATORY  
Washington, D.C.

SECURITY CLASSIFICATION OF THIS PAGE (When Data Entered)

REPORT DOCUMENTATION PAGE		READ INSTRUCTIONS BEFORE COMPLETING FORM
1. REPORT NUMBER NRL Memorandum Report 4086	2. GOVT ACCESSION NO. 14 NRL-MR-4086	3. RECIPIENT'S CATALOG NUMBER
4. TITLE (and Subtitle) 6 A UNIQUE RADIO OCEANOGRAPHIC RADAR .	5. TYPE OF REPORT & PERIOD COVERED 9 Final Report .	6. PERFORMING ORG. REPORT NUMBER
7. AUTHOR(s) 10 James E. Kenney and Edward J. Walsh	8. CONTRACT OR GRANT NUMBER(s) 15 NASA-L17098A	
9. PERFORMING ORGANIZATION NAME AND ADDRESS Naval Research Laboratory Washington, DC 20375	10. PROGRAM ELEMENT, PROJECT, TASK AREA & WORK UNIT NUMBERS NRL Problem G01-05.601	
11. CONTROLLING OFFICE NAME AND ADDRESS NASA Advanced Applications Flight Experiment Program Langley, Virginia	12. REPORT DATE 11 November 1979	
14. MONITORING AGENCY NAME & ADDRESS (if different from Controlling Office) NASA Wallops Flight Center Wallops Island, Virginia 23337 12 26	13. NUMBER OF PAGES 25	15. SECURITY CLASS. (of this report) UNCLASSIFIED
16. DISTRIBUTION STATEMENT (of this Report) Approved for public release; distribution unlimited.		
17. DISTRIBUTION STATEMENT (of the abstract entered in Block 20, if different from Report)		
18. SUPPLEMENTARY NOTES *NASA Wallops Flight Center, Wallops Island, Virginia		
19. KEY WORDS (Continue on reverse side if necessary and identify by block number) Directional spectra      Surface contour radar Real time computations      Surface height distribution Two dimensional FFT		
20. ABSTRACT (Continue on reverse side if necessary and identify by block number) A 36 GHz computer controlled airborne radar has been developed by NRL and NASA WFC which generates a false-color coded elevation map of the sea surface below the aircraft in real-time and can routinely produce ocean directional wave spectra with off-line data processing.		

DD FORM 1 JAN 73 1473

EDITION OF 1 NOV 65 IS OBSOLETE  
S/N 0102-014-6601

251 950  
SECURITY CLASSIFICATION OF THIS PAGE (When Data Entered)

## CONTENTS

I.	INTRODUCTION . . . . .	1
II.	SYSTEM DESCRIPTION . . . . .	1
III.	OBSERVATIONAL RESULTS . . . . .	5
IV.	OTHER APPLICATIONS . . . . .	9
V.	SYSTEM ADVANTAGES . . . . .	11

Accession For	
NTIS GRA&I	<input checked="" type="checkbox"/>
DDC TAB	<input type="checkbox"/>
Unannounced	<input type="checkbox"/>
Justification _____	
By _____	
Distribution/ _____	
Availability Codes	
Dist	Avail and/or special
A	

## A UNIQUE RADIO OCEANOGRAPHIC RADAR

### I. INTRODUCTION

The generation of a reliable model to predict sea state is very difficult due to the lack of observational inputs. Sufficient observations are impossible by conventional methods, especially for the most interesting cases of high sea state. Furthermore, almost all conventional methods are incapable of providing directional information about the wave field, which is a crucial parameter in wave propagation. The Surface Contour Radar (SCR), developed by the Naval Research Laboratory (NRL) and the NASA Wallops Flight Center (WFC) under the NASA Advanced Applications Flight Experiment (AAFE) program is readily capable of supplying directional wave height spectra.

### II. SYSTEM DESCRIPTION

The SCR is a beam-limited bistatic radar employing frequency diversity (35.7 GHz and 36.3 GHz). The SCR uses a digital bi-phase pulse compression technique to achieve selectable range resolutions of 0.15, 0.30, 0.61, 1.51 meters. Figure 1 shows the manner in which data are acquired. A horn fed lens illuminates an elliptical flat plate which oscillates back and forth to scan a  $1.2^\circ$  beam along the surface of the earth, within  $\pm 15^\circ$  of the normal to the aircraft wings, in a plane perpendicular to the aircraft's flight path. A fan-beam

Note: Manuscript submitted June 29, 1979.

antenna, with a half power beamwidth of  $1.2^{\circ} \times 40^{\circ}$ , receives the returning signal resulting in a two-way antenna beamwidth of  $0.85^{\circ} \times 1.2^{\circ}$ .

The SCR is capable of obtaining directional wave height spectra in any sea condition. Nominally, the aircraft altitude is adjusted so that the radar swath width is equal to seven times the dominant ocean wavelength ( $\lambda$ ) with an along-track resolution of  $0.2 \lambda$  and a data point spacing of  $0.1 \lambda$ . The radar provides a direct measurement of both the surface elevations and the relative intensities of the radar backscatter within its swath width. Figure 2 illustrates the system geometry as a function of altitude.

The directional wave spectra is obtained by applying a two-dimensional Fast Fourier Transform (FFT) to the SCR data. A highly desirable feature of the radar is that as the wave height increases, the observational altitude for the optimum tradeoff between along-track resolution (to resolve surface wavelength) and swath width (to resolve directional information) also increases.

Sea surface elevation is calculated in real time, false color coded, and displayed on a 48-cm color display. The elevation computation is illustrated in Figure 3. The computer

interacts with the radar hardware once for each lateral scan of the transmitter beam. As the antenna beam is scanned laterally, the range is scanned in and out in a predetermined sawtooth pattern which depends on the roll attitude of the aircraft and is designed to keep the region interrogated symmetric with respect to the mean sea level. Data is taken within a  $30^{\circ}$  sector of the antenna scan at  $0.6^{\circ}$  intervals. This results in 51 range scan legs. On each of the 51 range scan legs that make up the sawtooth pattern. The video signal is digitized for each range cell and that value is both accumulated and multiplied by its associated range number referenced to the start of the leg. That product is also summed. At the end of each range scan leg, the sum of the powers from each range (ISP), the sum of the range weighted powers (ISKP), and a number indicating the position on the leg where the return signal first exceeded a fixed threshold are stored in a data memory. The data memory is a first-in, first-out device (FIFO) that is 16 bits by 255 bits. Since the computer is a 16-bit machine, ISP and ISKP are divided into two 16-bit words and the threshold count becomes a fifth 16-bit word. During each lateral scan of the antenna beam, data is saved from the 51 range scan legs in the form of five 16-bit words which fill the FIFO. At the end of each lateral scan,

the 255 words are transferred into the computer where each ISKP is divided by the associated ISP to determine KBAR, the centroid of power for that leg of the range scan.

Figure 3 shows a portion of the range scan pattern and indicates the computation of the surface elevation, IELEV(N), where N is an index indicating which of the 51 range scan legs is under consideration. When the scan patterns were precomputed during the start-up phase, the range to the beginning of each leg, IR(N), was stored in the computer, as well as the cosine of the angle of that point from nadir. The range to the centroid of the return power is then found by adding or subtracting KBAR from IR(N). (Range decrements on odd numbered legs and increments on even numbered legs.) The cosine of the angle off-nadir corresponding to the centroid of the return power is found by linearly interpolating between the values at the end points of the leg using the ratio of KBAR to the total number of steps in that leg. The actual computations employ the cosine complement, (1-cosine), multiplied by 100,000 so that high accuracy may be maintained using integers while keeping the values below the 32,768 computer limit on the magnitude of an integer. The computer multiplies the range by the cosine of the angle to determine the vertical distance to the surface and subtracts that quantity from the nominal aircraft altitude, IH, to determine the surface elevation with respect to the reference level.

### III. OBSERVATIONAL RESULTS

Figure 4 shows data for a 5.5 m Significant Wave Height (SWH) sea with the aircraft flying perpendicular to the wave crests. The left hand part of the display is the elevation map with each color change representing an elevation change of 0.9 meters. The aircraft has a nominal stable flight air speed of approximately 75 m/s. It can be deduced from the aircraft ground speed (GS) and drift angle (DA), which are displayed in the graphics in Figure 4, that the aircraft is headed very nearly into the wind. There are 100 scan lines displayed with the top line being the most recent and the bottom line being the oldest. The waves are propagating from top right to bottom left of the display. The range resolution (RES) is 1 ns as indicated by the graphics. There are 60 elements in the color bar at the top of the figure. For Figure 4 each color in the color bar is 3 range cell units wide (0.45 meters) and a contour interval (CI) of 2 has been assigned. Therefore, a change in color represents an elevation change of 6 range cell units or 0.9 meters. The colors are in pairs and a change from light to dark denotes a decrease in elevation. The elevation information is permitted to wrap around in the color bar. By counting the color changes, it can be seen that the crest to trough elevation change of the wave is approximately 8 meters.

As shown in the graphics, the antenna is scanning at 15.9 lines per second (L/S). The display represents approximately 6 seconds of data and contains 100 lines and 5100 data points.

The black dots represent data dropouts, return signals that are too weak to process. The along-track surface dimension (330 meters) can be arrived at by multiplying time in seconds by ground speed (GS) in meters per second. Cross-track dimension (223 meters) is  $1/2$  the aircraft altitude. The wavelength in this figure is 140 meters and the ratio of wavelength to SWH is 25.4. Forecasts had predicted surface winds of 30 knots with gusts to 45 knots and the wind had been blowing in excess of 30 hours. Most of the data on 27 April was taken in a torrential rainstorm.

The right-hand side of Figure 4 shows the relative radar backscattered power normalized within each off-nadir angle interval. The color-coding order starts at the left in the color bar. Deep orange, at the far left of the color bar, represents a return signal power that is less than 50 percent of the mean power returned at that angle off-nadir. Light orange represents a return signal power between 50 and 100 percent of the mean power return at that same angle off-nadir. Each succeeding color represents an additional 50 percent signal return above the mean power at the same angle off-nadir.

Figure 5 shows a segment of data on the same day flying crosswind. The aircraft was aligned crosswind by

maximizing the drift angle. The crests and troughs appear to orient themselves from top right to bottom left, instead of the naturally assumed top to bottom.

This resulted from a combination of effects: (1) the wind direction changed with altitude, and (2) the large drift angle of the aircraft ( $18.9^{\circ}$ ) meant that the beam was not scanned perpendicular to the aircraft's ground track. The phase velocity of the ocean waves was approximately 14 m/s. The wind velocity at the aircraft's altitude was approximately 24 m/s. The waves would seem to drift to the right relative to the aircraft, although they actually were propagating towards the left. These effects are enhanced by a 20 percent compression in the vertical dimension of the display relative to the horizontal dimension for the particular set of parameters. Figures 6 and 7 show the directional spectra contours for the two different flight paths. Figure 6 displays the wave height spectra contours for the crosswind flight path while Figure 7 represents the upwind flight condition. The spectra have been normalized with the contours representing 10 percent intervals relative to the spectral peak. The dashed contour represents the 50 percent power level. In each of the figures the mirror image of the spectra is also displayed. The spectra in the two figures were calculated from data taken at an aircraft altitude that resulted in a cross-track swath of approximately 1.6 ocean

wavelengths rather than the desired seven wavelengths indicated in Figure 1. This resulted in some distortion in the cross-track information. On this particular day, Air Traffic Control had placed altitude constraints on the operation that resulted in the less than optimum conditions. However, even under these constraints, if data are taken in orthogonal directions and the resulting spectra averaged the determination of the directionality can be greatly improved.

Figure 8 shows the directional spectra for a 1.9 meter SWH condition when the flight path was nearly perpendicular to the crests. Along with the 41 meter wavelength energy, there is also a swell whose apparent wavelength is nearly 400 meters. The daily log indicates that there was a visible swell coming from the southeast.

The apparent wavelengths of the waves will be distorted due to the wave velocity relative to the aircraft velocity. The apparent wavelengths of waves traveling in the opposite direction as the aircraft will appear shortened and those of waves traveling in the same direction will appear lengthened. The effect is more pronounced for longer wavelengths since their phase velocity is higher. This effect is calculable and correctable, but it has not been removed from the spectra.

A slice of data taken out of the center of the swath width of the radar is compared with a profile taken by the NASA WFC Airborne Oceanographic Lidar (AOL) laser system in Figure 9. The AOL, which was also developed under the NASA AAFE program, is installed in the same aircraft and the two profiles are time coincident. The laser had a spot size of  $\approx 1/6$  meter, while the SCR spot size was 3.4 meters. The figure demonstrates good agreement between the instruments.

#### IV OTHER APPLICATIONS

An important oceanographic aspect of the SCR in contrast to the Synthetic Aperture Radar (SAR) is that the SCR produces direct range measurements that are converted in real time to sea surface elevations. The SAR measurement is indirect in that it is essentially a microwave photograph of the sea surface. The sea state conditions are inferred from the intensity of the reflected radiation but the backscattering mechanisms are still not completely understood. Since the SCR simultaneously acquires both elevation and intensity information, it should be invaluable in evaluating and more completely understanding the interpretation of SAR information.

The simultaneous acquisition of elevation and back-scattered power has already been used to determine the electromagnetic bias that affects a satellite radar altimeter's ability to measure the geoid in the presence of

a high sea state. Figure 10 shows histograms of the sea surface height distribution and radar backscattered power for two different values of SWH, 1.9 m and 5.5 m. The departure from mean sea level has been normalized by the surface height standard deviation in each case and a normal curve is indicated by dots for the sake of comparison. The radar backscatter distribution (dashed line), which is what an altimeter would see, is shifted towards the troughs (to the left) relative to the geometric mean in both cases. The magnitude of the shift is one to two percent of the SWH.

This system can also be used to generate very accurate relief maps of land areas which would include trees and man-made obstructions. The cross-track scan generated by the oscillating mirror would not contain any error due to aircraft vertical motion since the scan time is so short. There could be some errors induced in the along-track information due to inaccuracies in determining the aircraft's vertical motion. However, by flying a rectangular grid with flight lines spaced at half the swath width, the cross-track scan for one set of flight lines could be used to zero-set the along-track variation for the perpendicular set of flight lines.

## V. SYSTEM ADVANTAGES

The advantages of the system are: (1) the low data rate, (2) the measurement is direct, (3) the data processing is straightforward and does not require tremendous amounts of computer time, with the result that (4) a relief map would be available soon after the flight. Intensity maps could be developed more easily than relief maps and could be used to study soil moisture. With somewhat more complex data processing, this system could obtain maps of crop heights by differencing the ranges of the returns from the ground and the tops of the crop, if the top return were sufficiently strong, or by using the AOL laser mapper to obtain the range to the tops of a crop and the Surface Contour Radar to obtain the range to the bottom.

# AAFE SURFACE CONTOUR RADAR

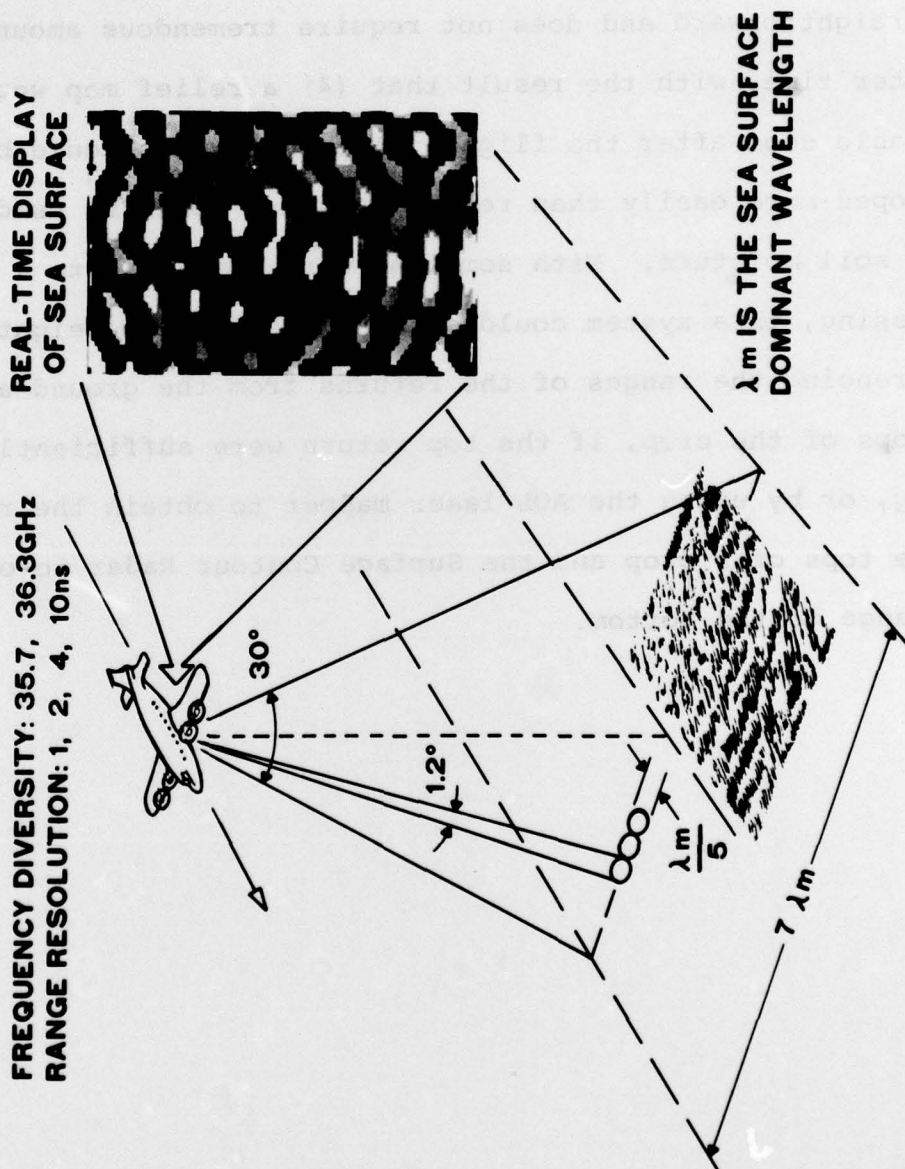


Fig. 1 — Measurement configuration

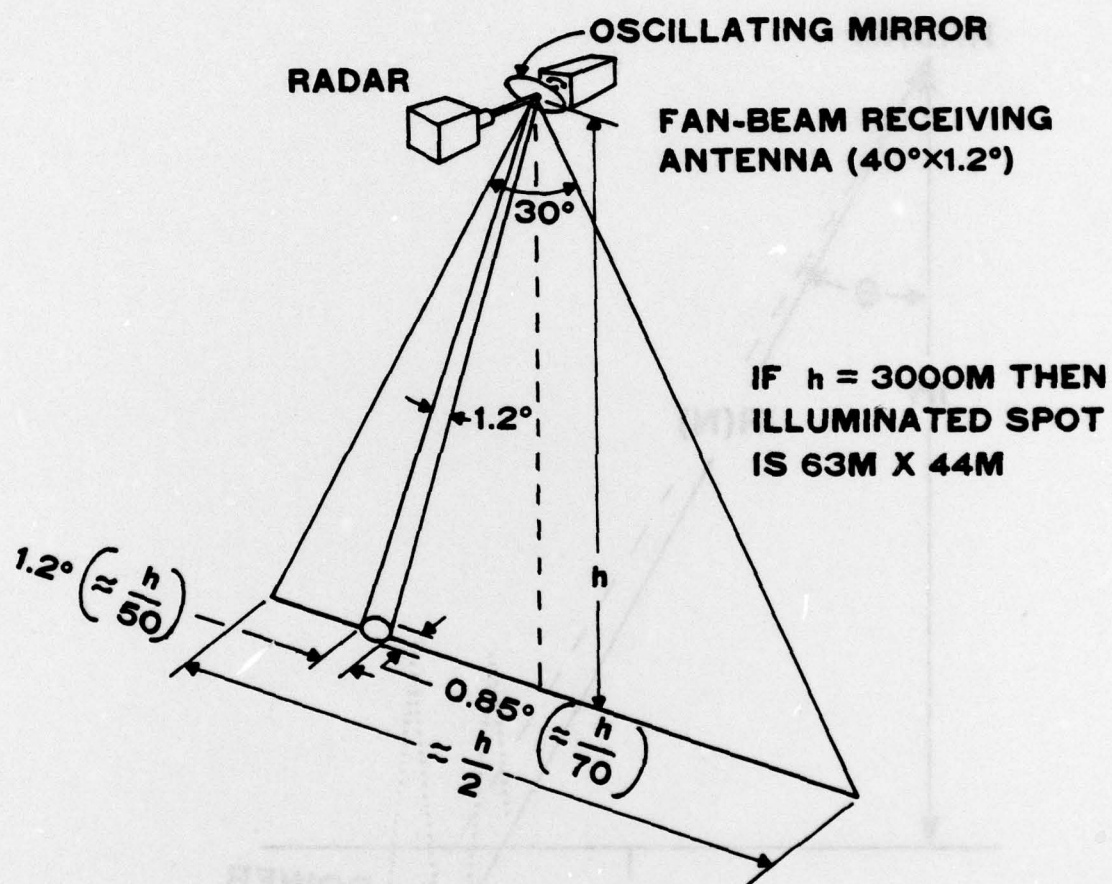


Fig. 2 - System geometry

$$IELEV(N) = IH - (IR(N) + (-1)^N KBAR) \cos \theta$$

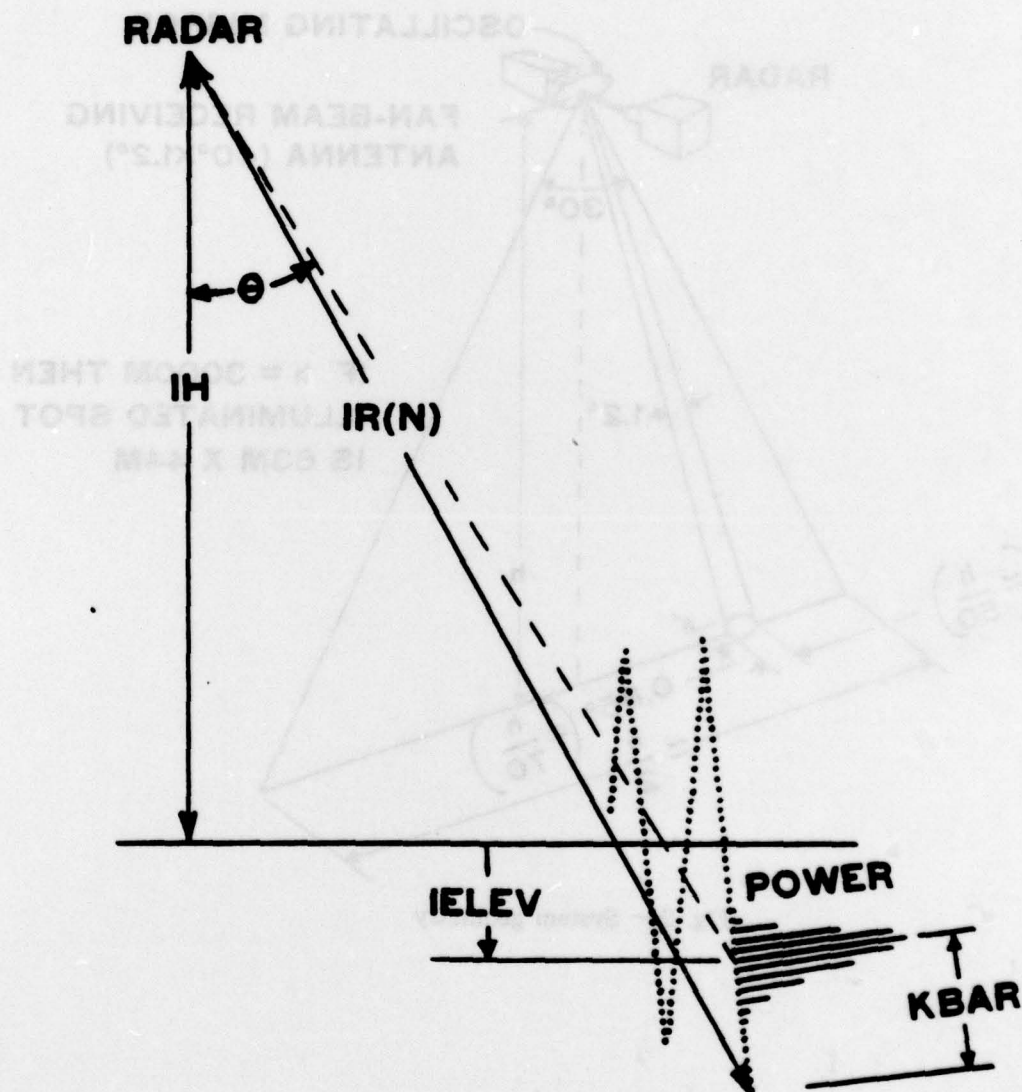


Fig. 3 - Sea surface height calculations

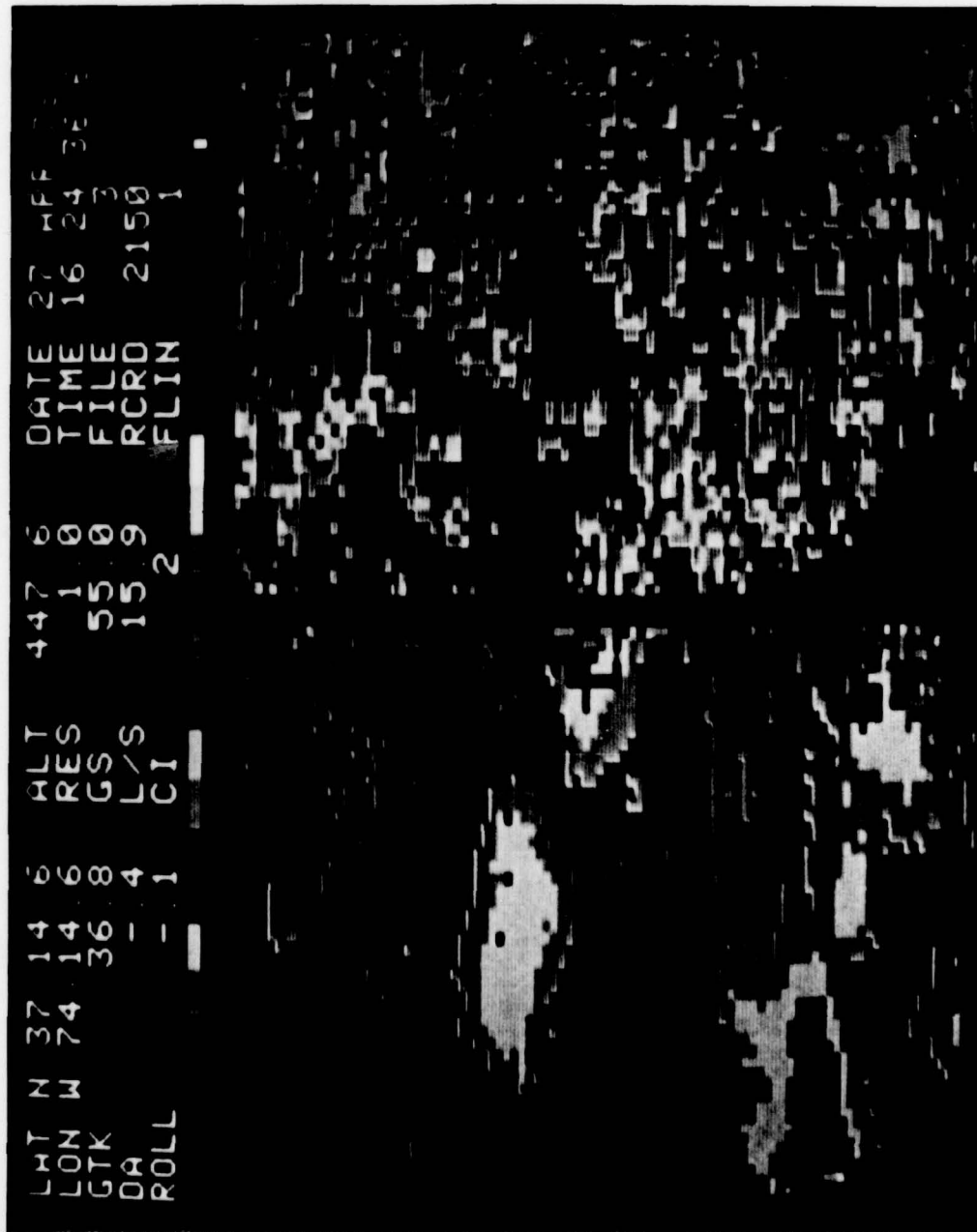


Fig. 4 — Real time display of ocean surface contour and relative backscattered power. The aircraft is flying into the wind.

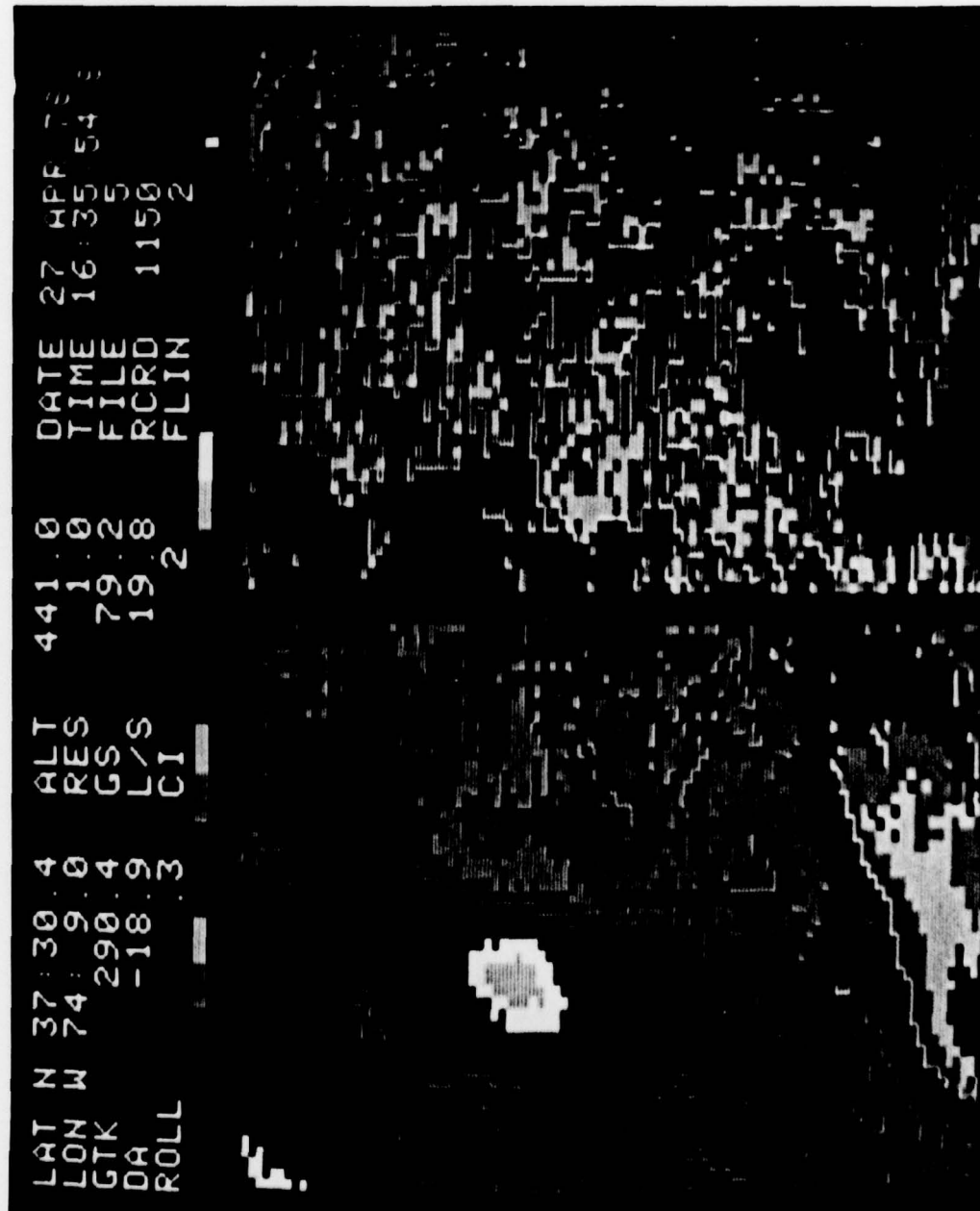
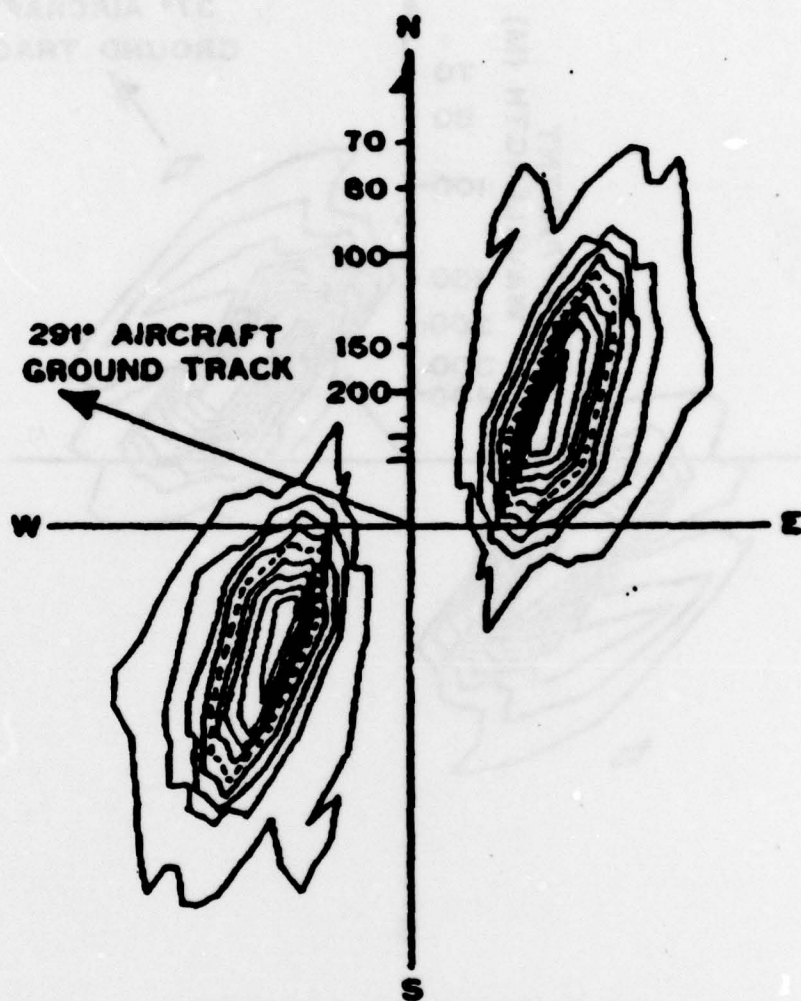
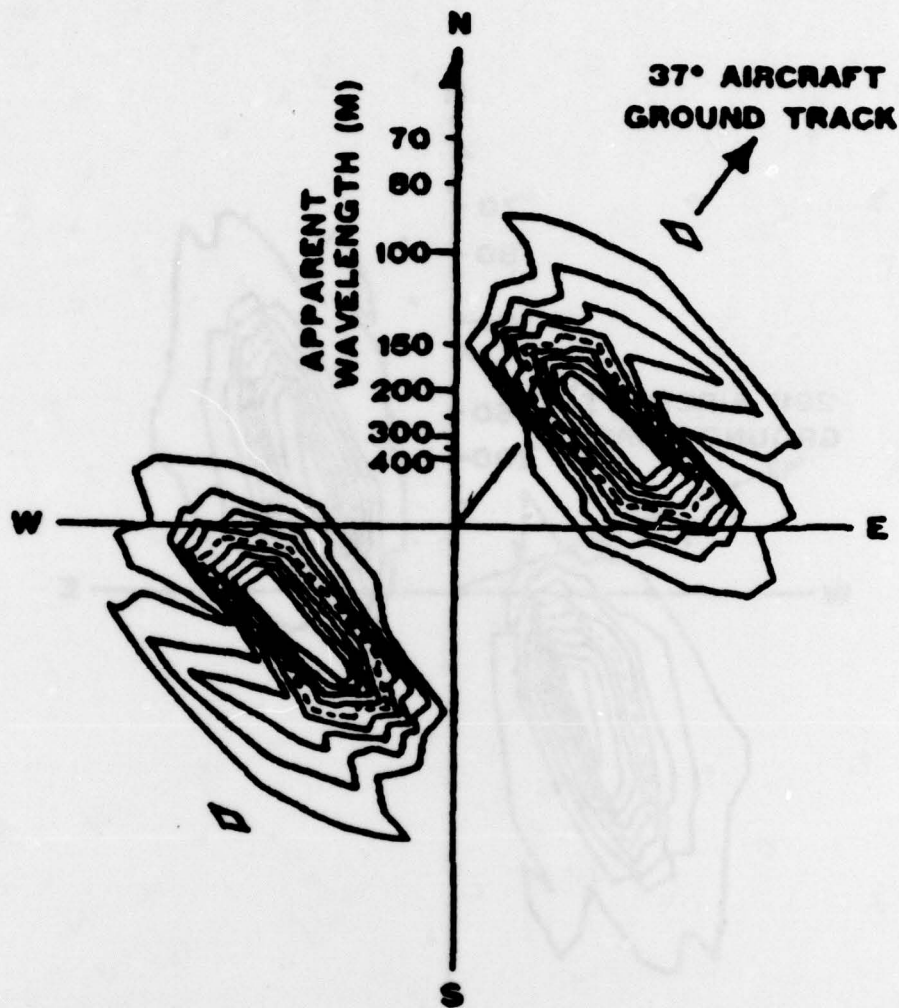


Fig. 5 -- Real time display of ocean surface contour and relative backscattered power. The aircraft is flying crosswind.



**440 M AIRCRAFT ALTITUDE**  
**5.5 M SWH**  
**140 M DOMINANT WAVELENGTH**

Fig. 6 — Ocean wave directional spectra with aircraft flying  
 crosswind 5.5 meter sea



**440 M AIRCRAFT ALTITUDE**

**6.5 M SWH**

**140 M DOMINANT WAVELENGTH**

Fig. 7 — Ocean wave directional spectra with aircraft flying into the wind 5.5 meter sea

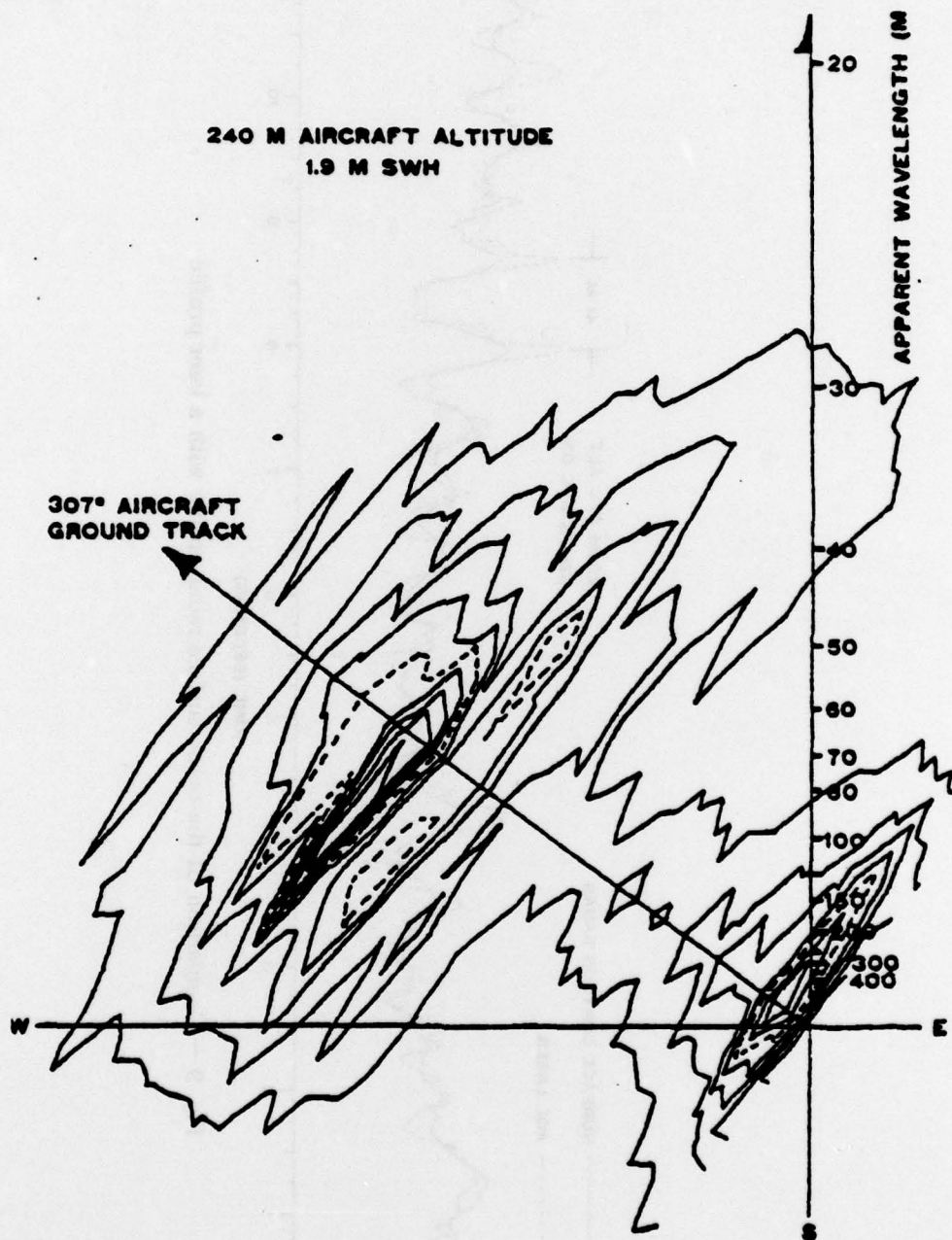


Fig. 8 — Ocean wave directional spectra with aircraft flying into the wind 1.9 meter sea

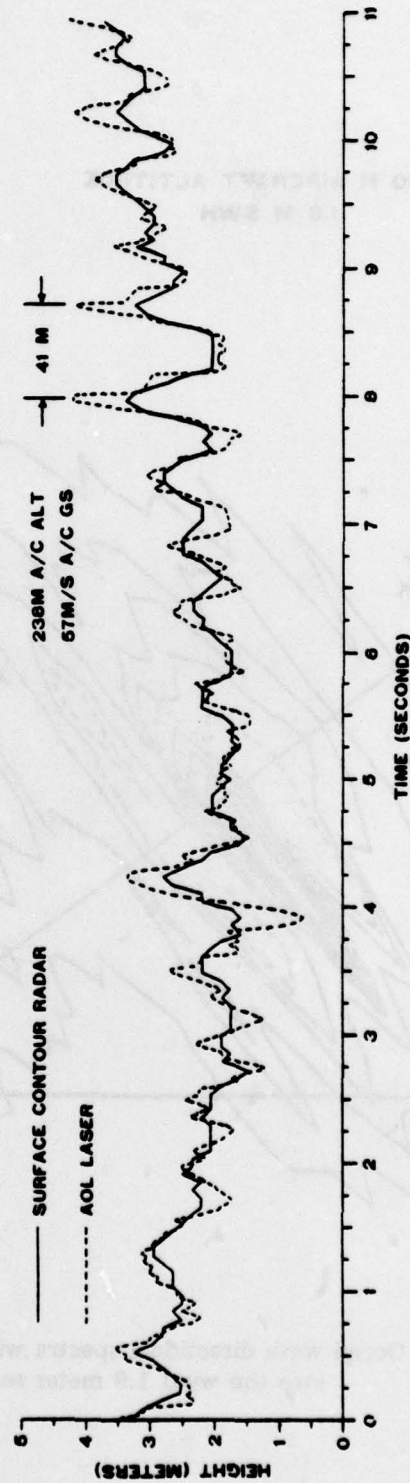


Fig. 9 — Comparison of the ocean surface radar profile with a laser profile

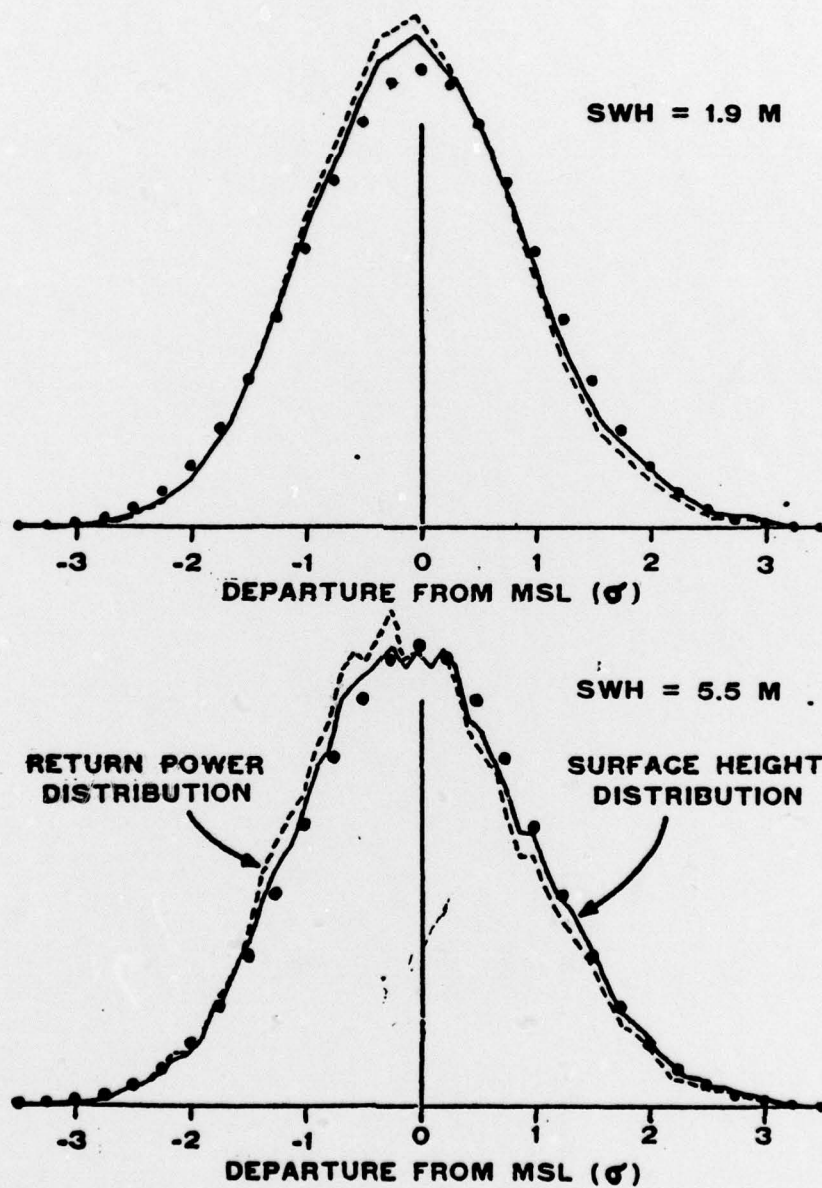


Fig. 10 — Ocean surface height distribution versus backscattered power distribution